Ocean Sci. Discuss., 12, 2073–2096, 2015
www.ocean-sci-discuss.net/12/2073/2015/
doi:10.5194/osd-12-2073-2015

Ocean Science
Discussions
Open Access

The role of vertical shear on the horizontal oceanic dispersion

A. S. Lanotte[1,2], R. Corrado[3], G. Lacorata[1], L. Palatella[1,2], C. Pizzigalli[1], I. Schipa[4], and R. Santoleri[3]

[1]CNR ISAC, GOS Team, Str. Prov. Lecce Monteroni, 73100 Lecce, Italy
[2]INFN, Sez. di Lecce, 73100 Lecce, Italy
[3]CNR ISAC, GOS Team, Via Fosso del Cavaliere 1, 00133 Rome, Italy
[4]ARPA Puglia (Regional Environmental Protection Agency), Corso Trieste 27, 70126 Bari, Italy

Received: 29 June 2015 – Accepted: 15 July 2015 – Published: 2 September 2015

Correspondence to: A. S. Lanotte (a.lanotte@isac.cnr.it)

Published by Copernicus Publications on behalf of the European Geosciences Union.

Abstract

The effect of vertical shear on the horizontal dispersion properties of passive tracer particles on the continental shelf of South Mediterranean is investigated by means of observative and model data. In-situ current measurements reveal that vertical velocity gradients in the upper mixed layer decorrelate quite fast (~ 1 day), whereas basin-scale ocean circulation models tend to overestimate such decorrelation time because of finite resolution effects. Horizontal dispersion simulated by an eddy-permitting ocean model, like, e.g., the Mediterranean Forecasting System, is mosty affected by: (1) unresolved scale motions, and mesoscale motions that are largely smoothed out; (2) poorly resolved time variability of vertical velocity profiles in the upper layer. For the case study we have analysed, we show that a suitable use of kinematic parameterisations is helpful to implement realistic statistical features of tracer dispersion in two and three dimensions. The approach here suggested provides a functional tool to control the horizontal spreading of small organisms or substance concentrations, and is thus relevant for marine biology, pollutant dispersion as well as oil spill applications.

1 Introduction

Tracer dispersion in the Ocean (Davis, 1983) has an impact on different environmental, chemical, biological and technological problems. Mean currents mostly contribute to large-scale transport, while small-scale motions tend to spread concentration fields or, equivalently, Lagrangian trajectories of passive or active tracers. In a nutshell, small-scale currents control the mixing and diffusion of substances or small organisms in the ocean.

The role of small-scale motion in geophysical flows is receiving a renewed attention, not only concerning the hydrodynamical modeling but also in relation to the biological consequences of specific phenomena. Recently, the statistics of odor detection during olfactory searches were studied, and the transport of pheromones by turbulent

OSD
12, 2073–2096, 2015

atmospheric flows was identified as a key factor to bring out the appropriate biological behavior of insects (Celani et al., 2014). Very little is known about the way turbulence and diffusion - in addition to other physical mechanisms-, model marine habitat and promote or impede the life of certain organisms (Ikawa et al., 1998).

Turbulence is thought to mostly have an homogenising effect, smearing sharp gradients and promoting super-diffusive separation in time of initially close trajectories: the relative diffusivity is expected to grow as the $4/3$ power of the separation distance $R(t)$, $D(R) \equiv \mathrm{d}\langle R^2(t)\rangle/\mathrm{d}t \sim R^{4/3}$, and the separation distance hence grows as $\langle R^2(t)\rangle \simeq t^3$, as suggested by Richardson in his pioneering work (Richardson, 1926; Falkovich et al., 2001). Laboratory experiments preferentially deal with homogeneous and isotropic flows: non-ideal and finite-size effects have then a limited impact, and measurements of turbulent dispersion do not show strong departure from statistical behaviour à la Richardson (Sawford, 2001; Salazar and Collins, 2009). Direct numerical simulations further supports these observations, additionally showing that deviations are rare and should be traced back to the intermittent nature of the flows (Biferale et al., 2014).

While the mathematical formulation of the problem of turbulent dispersion can be considered established (Bennett, 2005; Garrett, 2006), observations reported by experimental studies are much less clear (see e.g., LaCasce, 2010; Okubo, 1971; Morel and Larchevêque, 1974; Er-el and Peskin, 1981; Berti et al., 2011). This is only partly due to the inherent difficulties of performing float or dye concentration experiments in the ocean. Much of the uncertainty is due to the complex nature of the flow, and the relevance of non-ideal features associated to anisotropies and inhomogeneities, in addition to temporally or spatially local effects such as wind waves, tidal and inertial fluctuations.

From float trajectories analysis, Ollitrault and collaborators (2005) found that for pairs of particles, initially separated by a few kilometers, the relative diffusivity followed the $4/3$ law for separation distances between 40 and 300 km. At early times, and for smaller separations, they observed an exponential growth on a time-scale of about 6 days, but only for one of the two drifter clusters. The experiment was conducted in the central part of the North Atlantic where the Rossby internal radius of deformation is about 25 km. Coastal region experiments tend to support the existence of the exponential regime, but large uncertainties affect the observed mean dispersion properties (Ohlmann et al., 2012).

It is useful to recall that the Richardson 4/3 law can be observed also in the case of anisotropic relative dispersion, e.g. in the presence of a zonal mean shear and a meridional random walk (Bennett, 1987). More generally, any relative diffusion coefficient of the form $D(R,t) \sim R^{\alpha} t^{\beta}$, with $3\alpha + 2\beta = 4$, is dimensionally compatible with the mean squared separation growing as $\langle R(t)^2 \rangle \sim t^3$ (Monin and Yaglom, 1975), hence turbulence is not the only mechanism leading to the super-diffusive behaviour, $\sim t^3$.

Despite the rapidly increasing amount of experimental and numerical work devoted to the problem of ocean diffusion, a clear modeling framework well supported by experimental observations and numerical simulations is still lacking.

In this paper, we focus on the role of vertical shear as important mechanism promoting the horizontal diffusion in the ocean. When dealing with ocean diffusion, there is a huge experimental gap between buoyant/surface/two dimensional processes and three-dimensional ones. Indeeed the study of surface dispersion find an enormous help in the large amount of data coming from drifters deployed all over the ocean. These data can be considered the benchmark against which one can compare Lagrangian numerical simulations (Lacorata et al., 2014). Moreover the buoyant dynamics of the drifters is a good proxy for oil dispersion.

A complete different picture is encountered when dealing with three-dimensional Lagrangian diffusion. Measurements of current variation along the mixed layer are not so common, and are all mainly related to the use of Acoustic Doppler Current Profilers (ADCP). In order to simplify the problem, one could be tempted to use depth-averaged velocities for predicting horizontal dispersion, so neglecting shear effects. This approach can be misleading and have some important practical drawbacks in estimating the dispersion of 3-D tracers. The effect of vertical shear on the horizontal

OSD
12, 2073–2096, 2015

dispersion was first experimentally investigated in Okubo (1968, 1971). In LaCasce and Bower (2000), the effect of vertical shear on the horizontal dispersion of subsurface floats in the North Atlantic is discussed. On the basis of estimates inferred from the mean flow and *not* from the fluctuating velocities, vertical shear is expected to be much less important than horizontal shear for the oceanic diffusion.

From the numerical modelling point of view, being able to simulate Lagrangian dispersion in the ocean has great relevance: search and rescue problems, dispersal of biochemical tracers, oil spill, chlorophyll dynamics. It is however a delicate task because of the finite resolution of the circulation models, and more fundamentally because of the nonlinear character of the dynamics. When dealing with basin scale models, not only the mixed layer dynamics is often missing, but, also, the velocity field features from sub- to meso-scales are poorly resolved both temporally and spatially. At this regard, various techniques have been developed to model the small-scale velocity components which, nonetheless, play an important role during the early stage of tracer dispersion.

The approach here considered consists in the use of kinematic models (Palatella et al., 2014; Lacorata et al., 2014), which can be adapted to the different dispersion regimes, namely exponential separation, turbulent dispersion, standard diffusion. The kinematic model can be three dimensional, to simulate vertical convective motions in the ocean mixed layer, or two dimensional, to better account for the horizontal dispersion due to mescoscale eddies, very often underestimated in general circulation models. Here, we will discuss both situations.

The paper is organized as follows. In Sect. 2, we consider the relative dispersion properties of neutrally buoyant and three dimensional tracer particles and discuss the main statistical features through the technique of Finite Scale Lyapunov Exponent. In Sect. 3, we compare in-situ observations of vertical velocity gradients with those obtained from a general circulation model. Section 4 contains the final remarks.

OSD
12, 2073–2096, 2015

2 Lagrangian dispersion: the effect of vertical shear

We consider a neutrally buoyant tracer particle whose position is given by the three-dimensional vector $\boldsymbol{X}(t)$. The trajectory is assumed to evolve according to the Lagrangian equation

$$\frac{\mathrm{d}\boldsymbol{X}}{\mathrm{d}t}(t) = \boldsymbol{U}(\boldsymbol{X},t) + \boldsymbol{u}(\boldsymbol{X},t), \tag{1}$$

where the velocity field is simply decomposed in a large-scale term, $\boldsymbol{U}(\boldsymbol{x},t)$, and a small-scale contribution $\boldsymbol{u}(\boldsymbol{x},t)$. We consider the former, (U,V,W), as the resolved component in General Circulation Models (GCM), and the latter, (u,v,w), as the unresolved or poorly resolved component. Several authors have proposed in the past different recipes to model the small-scale motions (see e.g., Haza et al., 2007; Berloff and McWilliams, 2002). Later on, we shall come back on this point.

When considering Lagrangian dispersion, the problem is easily reformulated in terms of the time evolution of the pair separation vector $\boldsymbol{R}(t) \equiv \boldsymbol{X}_i(t) - \boldsymbol{X}_j(t)$, where $i,j = 1,\ldots,n$ indicate the tracer particles, and $i \neq j$:

$$\frac{\mathrm{d}\boldsymbol{R}}{\mathrm{d}t}(t) = \boldsymbol{\Delta}_R\boldsymbol{U}(\boldsymbol{R},t) + \boldsymbol{\delta}_R\boldsymbol{u}(\boldsymbol{R},t). \tag{2}$$

Hence two particles at mutual distance $R_0 = |\boldsymbol{R}(t=0)|$ start to separate because of a non-zero velocity fluctuations at that scale. Depending on the value of R_0 and on the local dynamics, such velocity fluctuations can be ascribed to very different flow motions. Let us consider the simple situation of two particles, $P1$ and $P2$, located in the ocean mixed layer and initially separated only along the vertical direction $\boldsymbol{R}_0 = (\simeq 0, \simeq 0, R_0)$. In the absence of vertical shear, and taking into account that vertical velocities are very small, these particles will keep their initial separation almost unchanged so that $R(t) \simeq R_0$. As a result horizontal diffusion will be very weak, if not zero. The situation is different when e.g. particles have the chance to experience for some time a mean vertical shear.

OSD
12, 2073–2096, 2015

If this is the case, $U(Z_1,t) \neq U(Z_2,t)$ and/or $V(Z_1,t) \neq V(Z_2,t)$, and particles will start separating. This is better illustrated in Fig. 1, which shows that vertical shear imply horizontal pair dispersion. It is clear that the vertical shear is bounded by two opposite situations: on one hand, a mean shear, i.e. a shear profile with very long correlation time as it happens for example in the presence of strong background currents; on the other hand, a fluctuating vertical shear due to turbulent motions and hence rapidly changing in time. As we will discuss in the Sect. 3, the situation in the mixed layer of the Mediterranean sea is in between these two extrema, and the typical time scale of persistent vertical shear profiles is of the order of one to few days.

The starting point of our quantitative analysis is to measure the statistical properties of dispersing tracer particles. For this, we want to compare data of numerical simulations of Lagrangian dispersion with direct measurements of drifters released in the Mediterranean, after (Lacorata et al., 2014). In Sect. 2.1, we detail the Lagrangian numerical simulations, while in Sect. 2.2, we compare experimental and numerical results.

2.1 Numerical simulations of Lagrangian dispersion

Lagrangian numerical simulations are performed using zonal and meridional components of the velocity field provided by the Mediterranean sea Forecasting System (MFS) model (Tonani et al., 2008), which uses the primitive equations with the Boussinesq, hydrostatic and incompressible approximations written in spherical coordinates. Grid resolutions are of $1/16^\circ \times 1/16^\circ$ degrees in the horizontal directions (≈ 6.5 km), and 72 vertical levels. The unevenly spaced levels have a thickness ranging from 3 m at the surface to 300 m at the bottom. The first level is 1.5 m deep and the last is about 5000 m deep. If we estimate the first internal Rossby radius of deformation of the order $O(10)$ km on average, then MFS is an eddy-permitting model for the Mediterranean Sea. Using Eq. (2), MFS velocity fields constitute the zonal $U(\boldsymbol{x},t) = U_{\mathrm{MFS}}$ and meridional $V(\boldsymbol{x},t) = V_{\mathrm{MFS}}$ components of the large-scale term, evaluated on model grid

OSD
12, 2073–2096, 2015

points; vertical component $W(\boldsymbol{x},t)$ is not explicitly available in MFS datafile considered, and we did not consider it.

In models such as the MFS, short-time and small-scale motions are lost because of coarse resolution. However, in transport and mixing processes, these unresolved fluctuations can be particularly relevant, even beyond the sub-grid scale. To take into account these components, we adopt a strategy in terms of a Lagrangian Kinematic Modelling (KLM) as described in Palatella et al. (2014) and Lacorata et al. (2014). Here we only recall a few elements that are essential for the present discussion. The velocity components of the KLM are defined as

$$\begin{aligned} u(\boldsymbol{X},t) &= \frac{\partial \Phi_1}{\partial z}, \\ v(\boldsymbol{X},t) &= -\frac{\partial \Phi_2}{\partial z}, \\ w(\boldsymbol{X},t) &= -\frac{\partial \Phi_1}{\partial x} + \frac{\partial \Phi_2}{\partial y}. \end{aligned} \tag{3}$$

In the above equations, the vector potential $\boldsymbol{\Phi}$, of components $(\Phi_1, \Phi_2, 0)$, is given by:

$$\begin{aligned} \Phi_1(\boldsymbol{x},t) &= \frac{A}{\widehat{k}} \sin[k(x - s\sin(\varpi t))] \sin[\widehat{k}(z - s\sin(\varpi t))], \\ \Phi_2(\mathbf{x},t) &= \frac{A}{\widehat{k}} \sin[k(y - s\sin(\varpi t))] \sin[\widehat{k}(z - s\sin(\varpi t))], \end{aligned} \tag{4}$$

and A is the velocity scale, $k = 2\pi/l_0$ is the horizontal wavenumber associated to the wavelength l_0 of the flow, $\widehat{k} = 2k$ is the vertical wavenumber assumed to be twice the horizontal wavenumber for isotropy, $t_c = l_0/A$ is the convective time scale; s and ϖ are amplitude and pulsation of the time-dependent oscillating terms. The velocity field in Eq. (3) is divergence-free by definition. Further, the suppression of the vertical dynamics below the mixed layer is included in the model in terms of a damping term

OSD
12, 2073–2096, 2015

$\Upsilon(z) = \exp(-|z|/L)$, multiplying the stream-functions Φ_1 and Φ_2. The exponential relaxation term guarantees that KLM velocities go to zero at depths much larger than the lenght scale L, being L of the order of the mixed layer depth.

In order to simulate the effect of a turbulent cascade, we superimpose n different kinematic modes. In particular for the three-dimensional KLM we use $n = 5$ with these values of parameters

$$\begin{cases} l_n = \{25.0, 33,4, 50.0, 70.7, 100\}\ \mathrm{m} \\ k_n = 2\pi/l_n;\ A_n = (\epsilon l_n)^{1/3}\ \mathrm{m\,s^{-1}} \\ \omega_n = 2\pi A_n/l_n; \\ L = 100\ \mathrm{m}, \quad \varepsilon = 10^{-5}\mathrm{m^2\,s^{-3}}. \end{cases} \tag{5}$$

Here ε is the turbulent dissipation rate that is used as main parameter of the turbulent cascade through the dimensional relation $v^3 \simeq L\varepsilon$ (Frisch, 1995). The two-dimensional KLM is used with the same parameterisation of Lacorata et al. (2014).

We performed three series of numerical simulations releasing $N_{\mathrm{pair}} \simeq 50\,000$ pairs of neutrally buoyant particles. In all series, pairs are initially homogeneously distributed in the whole Mediterranean Sea, 10 km offshore from the coast. An elastic collision takes place when particles meet the domain boundaries. Within each pair, particles start at the same latitude and longitude position, but they are vertically separated: one particle starts at $z = -3$ m below the surface, the other at $z = -43$ m, hence $\boldsymbol{R}_0 = (0, 0, 40)$. Simulations are carried out for one year (from 1 January to 31 December 2009), and integration time step is $\mathrm{d}t = 120$ s. The three series of simulation are so characterised:

- Series I: the KLM velocity is absent and particles keep their initial depth unchanged throughout the entire simulation. This is quite far from realistic conditions, however this numerical experiment is useful to quantify the effect of the vertical shear solely due to the mesoscale MFS model dynamics.

OSD
12, 2073–2096, 2015
The role of vertical shear on the horizontal oceanic dispersion
A. S. Lanotte et al.

- Series II: the KLM term is switched on, with the parameters shown in (Eq. 5). As a result of the presence of the sub-grid-scale dynamics, particles can also move vertically (between the surface and a depth scale of the order of L).
- Series III: it differs from the series II due to the fact that the 2-D KLM model is also added. The 2-D KLM is essential in simulating the mesoscale structures that are not completely resolved by the MFS model. As in Lacorata et al. (2014), parameters are tuned in order to numerically obtain an horizontal dispersion with the same statistical properties (more precisely the same Finite-scale Lyapunov Exponent) of the actual surface drifters (the points labelled as "Surface floats" in Fig. 2).

Next, we compare results from these runs with those obtained in Lacorata et al. (2014), where data of about 700 surface floats trajectories dispersing in the whole Mediterranean between 1990 and 2012 were studied.

2.2 Lagrangian dispersion: the Finite-Scale Lyapunov Exponent

The most natural way to quantify Lagrangian dispersion statistics is in terms of the moments $\langle \boldsymbol{R}^p(t) \rangle$, of the pair separation probability distribution function $P(\boldsymbol{R},t)$ (LaCasce, 2010; Biferale et al., 2014), measuring the probability to observe a pair separated by the distance vector $\boldsymbol{R}$ at time t. Standard obervables are the moment of order two, the mean square particle separation $\langle \boldsymbol{R}^2(t) \rangle$, and its time derivative, i.e., the relative diffusivity $D(\boldsymbol{R},t)$. Alternatively one can use the Finite-Scale Lyapunov Exponent (FSLE) (Boffetta et al., 2000). The advantage of this choice, often exploited in ocean dispersion applications (LaCasce, 2008), is that different dispersion regimes are disentangled and crossover effects are minimised. More details about the use of scale-dependent indicators in Lagrangian dispersion problems can be found in Berti et al. (2011).

The method consists of fixing a set of threshold scales, $\delta_n = \rho^n \delta_0$, where $\rho > 1$, $n = 1,2,3,\ldots$ and δ_0 can be chosen of the order of the initial pair separation. We then need to calculate the time, $T(\delta)$, it takes for the pair separation distance $R(t)$ to change

OSD
12, 2073–2096, 2015

from δ_n to δ_{n+1}. By averaging over the particle pair ensemble, we obtain the mean exit time, $\langle T_\rho(\delta_n)\rangle$, or mean *doubling time* if $\rho = 2$. Formally we are calculating the first passage time. The FSLE has the dimension of an inverse of time and is defined as

$$\lambda(\delta) \equiv \frac{1}{\langle T(\delta)\rangle} \ln \rho. \tag{6}$$

If $\delta \rightarrow 0$, the FSLE no longer depends on the scale and coincides with the Maximum Lyapunov Exponent on the flow: this happens when particles separate exponentially in time. For finite separations, if relative dispersion is governed by a $\langle R^2 \rangle \simeq t^\nu$ regime, then by dimensional analysis the FSLE is expected to scale as $\lambda(\delta) \simeq \delta^{-2/\nu}$. Most relevant regimes are the case of standard diffusion, for which we expect $\lambda(\delta) \simeq \delta^{-2}$; Richardson's diffusion, $\lambda(\delta) \simeq \delta^{-2/3}$; and ballistic or shear dispersion, with $\lambda(\delta) \simeq \delta^{-1}$.

Here, since we want to compare how the horizontal diffusion is influenced by the different flow realizations, in the FSLE we consider horizontal separations only.

In Fig. 2, we compare different measurements of the FSLE obtained from drifters and from numerical simulations. First, we observe that surface drifters and MFS surface tracers data show a striking difference: while at large scale they have the same behaviour, at a scale $\delta \simeq 40$ km they depart. In particular, for Lagrangian particles moving in the MFS velocity field, numerical simulations unrealistically suggest that it would take approximately the same time to reach a separation scale of the order of few kilometers and a separation scale ten times bigger. This discrepancy is due to both the coarse spatial resolution and the time averaging of any mesoscale model. Note that the scale at which MFS surface tracers deviate from drifters is larger that the model resolution: this suggests that scale resolution is quite crucial for Lagrangian statistics.

How does vertical shear affect these results? Can the vertical shear substantially modify horizontal dispersion? We address these questions using numerical data from Series I, II and III. The former clearly indicates that vertical shear is able to promote horizontal dispersion. Neutrally buoyant tracers moving at different depths experience velocity differences: as a result they start to separate already at very small scales.

OSD
12, 2073–2096, 2015

Results from Series II, where the KLM terms are switched on and particles vertically explore the whole mixed layer, are very similar to the former. This is somehow surprising, since the introduction of small-scale fluctuations does not substantially modify the horizontal pair dispersion: the dominant effect is the one associated to the vertical shear. Another important results is shown by the FSLE of series III that is larger than those of series II for all the scales. This means that the shear dispersion effect induced by the MFS currents is clearly detectable, but that it is lower than the dispersion induced by the mesoscale eddies inserted in the 2-D KLM.

We can summarise the results of the numerical simulations as follows. Adding vertical mixing to the ocean model, e.g. in the form of the 3-D kinematic model, may trigger a type of shear dispersion which is affected by an anomalous persistence of the vertical velocity gradients, as discussed in Sect. 3. On the other hand, comparing mesoscale dipersion of the MFS model with Mediterranean drifter data, one sees that real drifter pair dispersion follows a turbulent-like type of behavior, whereas model trajectories separate more slowly and at a nearly constant rate. Adding a two dimensional kinematic model, which can be easily set up to reproduce the main characteristics of the mesoscale drifter dispersion, one finds that: (1) the scale-dependent dispersion rates of numerical and drifter trajectories get very well compatible with each other; (2) the shear dispersion effects become practically negligible, being hidden by the more energetic turbulent-like dispersion processes occurring at the mesoscales.

Such observations open the second part of the paper: namely, trying to quantitatively assess the statistical features of the vertical shear. In the following, this is done for the specific case of the continental shelf of South Mediterranean for which we have in-situ measurements.

3 Vertical shear statistics: experimental versus numerical data

We analyse the vertical velocity profiles recorded with two Acoustic Doppler Current Profilers (ADCP) working at 300 kHz. These have been deployed on the continental shelf of the South Mediterranean: the first one is located at the following position: 31.91° N, 30.58° E, the second one at the close position 31.92° N, 32.00° E. Both instruments are bottom-mounted at the depth of 104 m; currents are uniformly measured between $Z = -13$ and $Z = -93$ m, the spacing is $\delta Z = 4$ m. Measurement records cover the period from 1 February 1999 until 11 February 2000. We analyzed data separating them into two time intervals: *I1*, from February 1999 until April 1999; *I2* from December 1999 until February 2000. In both periods, the thermocline is about 80 m deep. Figure 3 shows three examples of the recorded profiles, together with the ADCPs location.

In-situ measurements are compared with MFS current data extracted at the same locations, and for the same period; it is useful to recall that MFS data are daily.

Being our interest on the vertical shear, we adopted the following procedure:

- we first remove the mean velocity components from the current measurements at different levels, $U(Z,t)$ and $V(Z,t)$;

- for each δz, the vertical velocity gradient time series are constructed as $\gamma_x(Z,t) = [U(Z,t) - U(Z-\delta Z,t)]$, and $\gamma_y(Z,t) = [V(Z,t) - V(Z-\delta Z,t)]$;

- velocity gradient residual times series, $\gamma'_x(Z,t)$ and $\gamma'_y(Z,t)$, are obtained by removing the mean gradient, estimated over the whole time series.

We first calculate the auto-correlation function $C_{x,y}(\tau)$ separately for each velocity gradient component as

$$C_{x,y}(\tau) \equiv \frac{\langle [\gamma'_{x,y}(t_0+\tau)\gamma'_{x,y}(t_0)] \rangle}{\langle [\gamma'_{x,y}(t_0)]^2 \rangle}, \tag{7}$$

where the average is performed over different choices of the initial record t_0, and over few depths between $Z = -20$ and $Z = -50$ m, to gain statistical accuracy. Currents at lower and larger depths have not been considered.

OSD
12, 2073–2096, 2015

In Fig. 4, we compare the auto-correlation functions obtained from the ADCP with those of the MFS fields for the same days and the same locations. Data exhibit specific behaviour depending on the location and on the averaging period. However, general features can also be found. The ADCP $C_{x,y}(\tau)$ curves are oscillatory, which makes the determination of the correlation time

$$\mathcal{T}_\mathrm{c} = \int_0^\infty C(\tau)\,\mathrm{d}\tau \tag{8}$$

quite difficult. In the absence of a well converged integral, a possible choice is to estimate the value of $\mathcal{T}_\mathrm{c}$ from the time lag at which the curve attains the value 0.1. Clearly such extrapolation is quite rough and an error of the order of 10 % should be considered. ADCP data show that vertical shear components usually persist over a correlation time $\mathcal{T}_\mathrm{c}^\mathrm{ADCP} \simeq 0.5$ day or less.

For MFS curves, the situation is rather different: in one case, the curve never really attains zero; in the other case, it does on a time lag $\mathcal{T}_\mathrm{c}^\mathrm{MFS} \simeq 5$ days, so about ten times bigger. This observation suggests that at least this GCM might overestimate the temporal persistency of velocity gradients, unrealistically increasing the effect of the shear on the horizontal dispersion.

Finally, in Fig. 5, we examine the behavior of the probability distribution functions of the vertical shear components; they are normalised to have unit variance. We compare the PDF as extracted from the ADCP at 31.92° N, 32.00° E, averaging over the periods *I1* and *I2*, and similarly we do for MFS data interpolated at the same location. If we directly compare ADCP with MFS data, it appears that the former has a larger variance, which is clearly associated to the fact that MFS data lose small-scale and fast variability. Additionally, ADCP probability density function has fat tails, the fingerprint of a turbulent-like dynamics. Taking into account such variability can be important for Lagrangian modellisation of ocean dispersion processes. However if we compare daily averaged ADCP with MFS data, the cores of the unitary variance PDFs are very similar

OSD
12, 2073–2096, 2015

(not shown): this implies that for not too intense fluctuations, experimental ADCP and numerical MFS data account for the same kind of dynamics.

4 Conclusions

In this paper, we have discussed the effect of vertical shear onto the horizontal pair dispersion of tracer particles on the continental shelf of South Mediterranean. Coastal regions are very often affected by strong anthropogenic pressure due to waste water coming from coastal cities, and to the load of pollutant of river discharges (DiGiacomo et al., 2004; Israelsson et al., 2006). A good estimate of the Lagrangian dispersion rate at different spatial scales is important in evaluating and mitigating potentially harmful effects on the environment. Continental shelves and coastal regions are key places for the biological activity. For example, chlorophyll typically develops near the coasts, to be then advected and dispersed along the current with a vertical distribution that extends across the whole mixed layer. Also, vertical shear has been recently identified as a key ingredient to explain the strong small-scale patchiness of motile phytoplankton (Durham et al., 2013; Santamaria et al., 2014).

Here, we have specifically addressed the problem of simulating horizontal tracers dispersion, assuming that the tracer can be considered as passive, i.e. motility is absent and there is no feedback on the flow dynamics. A limit case is when the tracer particles or the concentration field are constrained to a two dimensional surface.

Numerical simulations with the MFS model show that, differently from drifters, pairs released at the same depth tend to exponentially separate with a dispersion rate nearly constant over a wide range of scales, up to the mesoscales. At larger scales (> 100 km), as soon as spatial correlations decay, the relative dispersion tends to a diffusive regime. However, if two trajectories having the same initial position are shifted in the vertical direction, then the horizontal dispersion rate grows as the separation tends to zero: it is the effect of the vertical gradient of the horizontal velocities.

OSD
12, 2073–2096, 2015

This observation implies that, at spatial scales smaller or comparable with the mixed layer size, shear dispersion can be quite important. Its relevance might be under or overestimated depending if vertical gradients of the current field change too fast or are anomalously persistent in time, rispectively. To verify if this is the case, we have analysed the statistical properties of vertical velocity gradients from field experiments, and from MFS numerical simulations in the specific region of the continental shelf of South Mediterranean. Differences arise both for the magnitude and for the temporal behaviour. In particular, the velocity gradients autocorrelation functions of ADCP data possess a characteristic time scale that is much smaller than that of the model: hence, numerical pair trajectories, on average, separate because of a vertical shear effect that lasts too long compared to the actual mixed layer conditions. In other words, temporal coherence of vertical shear is overestimated, and so its effect on pair dispersion.

Kinematic modelling, here exploited with both 2-D and 3-D sub-grid-scale parameterisations, substantially modifies the horizontal dispersion. In particular, since actual shear dispersion is lower than or comparable to those obtained by the MFS, we can argue that the MFS model plus the 3-D and 2-D KLM is a good modeling chain able to recover the correct relative Lagrangian dispersion at all scales larger than few km.

A different possibility, yet to be explored, is to build up an ad hoc *Lagrangian* small-scale kinematic model accounting for the locally homogeneous shear-dominated dynamics, similarly to what has been done with the shear-improved sub-grid-scale models in the *Eulerian* framework (Lévêque et al., 2007). Future ocean experiments focusing on the dispersion properties of tracers having vertical structures, such as the chlorophyll field, are needed to reveal more about the dynamics and statistics at those spatial scales where shear might dominate.

Acknowledgements. This work has been supported by SSD PESCA and RITMARE Research Projects (MIUR-Italian Research Ministery). This study has been conducted using MyOcean Products, that we acknowledge. The MFS current data are retrieved from MyOcean as MED-SEA_REANALYSIS_PHYS_006_004 myov04-med-ingv-cur-rean-dm. ADCP data were kindly delivered by the Italian *Ente Nazionale Idrocarburi* (ENI SpA). These data are collected as part of an industry-sponsored initiative and are currently proprietary. Technical support by Ing. F. Grasso at ISAC Lecce is kindly acknowledged.

References

Bennett, A. F.: A Lagrangian analysis of turbulent diffusion, Rev. Geophys., 25, 799–822, 1987. 2076

Bennett, A. F.: Lagrangian Fluid Dynamics, Cambridge University Press, Cambridge, UK, 2005. 2075

Berloff, P. and McWilliams, J.: Material transport in Oceanic gyres – Part 2: Hierarchy of stochastic models, J. Phys. Ocean., 32, 797–830, 2002. 2078

Berti, S., Alves Dos Santos, F., Lacorata, G., and Vulpiani, A.: Lagrangian Drifter Dispersion in the Southwestern Atlantic Ocean, J. Phys. Ocean., 41, 1659–1672, 2011. 2075, 2082

Biferale, L., Lanotte, A. S., Scatamacchia, R., and Toschi, F.: Intermittency in the relative separations of tracers and of heavy particles in turbulent flows, J. Fluid Mech., 757, 550–572, 2014. 2075, 2082

Boffetta, G., Celani, A., Cencini, M., Lacorata, G., and Vulpiani, A.: Non-asymptotic properties of transport and mixing, Chaos, 10, 50–60, 2000. 2082

Celani, A., Villermaux, E., and Vergassola, M.: Odor Landscapes in Turbulent Environments, Phys. Rev. X, 4, 041015, doi:10.1103/PhysRevX.4.041015, 2014. 2075

Davis, R.: Oceanic property transport, Lagrangian particle statistics, and their prediction, J. Mar. Res., 41, 163–194, 1983. 2074

DiGiacomo, P. M., Washburnb, L., Holta, B., and Jonesc, B. H.: Coastal pollution hazards in southern California observed by SAR imagery: stormwater plumes, wastewater plumes, and natural hydrocarbon seeps, Marine Poll. Bull., 49, 1013–1024, 2004. 2087

Durham, W., Climent, E., Barry, M., De Lillo, F., Boffetta, G., Cencini, M., and Stocker, R.: Turbulence drives microscale patches of motile phytoplankton, Nat. Comm., 4, 2148, doi:10.1038/ncomms3148, 2013. 2087

Er-el, J. and Peskin, R.: Relative diffusion of constant-level ballons in the southern hemisphere, J. Atmos. Sci., 38, 2264–2274, 1981. 2075

Falkovich, G., Gawędzki, K., and Vergassola, M.: Particles and fields in fluid turbulence, Rev. Mod. Phys., 73, 913–975, 2001. 2075

Frisch, U.: Turbulence, the legacy of A. N. Kolmogorov, Cambridge University Press, Cambridge, UK, 1995. 2081
Garrett, C.: Turbulent Dispersion in the Ocean, Prog. Ocean., 70, 113–125, 2006. 2075
Haza, A. C., Piterbarg, L., Martin, P., Ozgokmen, T. M., and Griffa, A.: A Lagrangian subgrid-scale model for particle transport improvement and application in the Adriatic Sea using the Navy Coastal Ocean Model, Ocean Mod., 7, 68–91, 2007. 2078
Ikawa, T., Okubo, A., Okabe, H., and Cheng, L.: Oceanic diffusion and the pelagic insects Halobates spp. (Gerridae: Hemiptera), Mar. Biol., 131, 195–201, 1998. 2075
Israelsson, P., Young Do, K., and Adams, E.: A comparison of three Lagrangian approaches for extending near field mixing calculations, Envir. Mod. Soft., 21, 1631–1649, 2006. 2087
LaCasce, J. H.: Statistics from Lagrangian observations, Prog. Ocean., 77, 1–29, 2008. 2082
LaCasce, J. H.: Relative displacement probability distribution functions from balloons and drifters, J. Mar. Res., 68, 433–457, 2010. 2075, 2082
LaCasce, J. H. and Bower, A.: Relative dispersion in the subsurface northatlantic, J. Mar. Res., 58, 863–894, 2000. 2077
Lacorata, G., Palatella, L., and Santoleri, R.: Lagrangian predictability characteristics of an Ocean Model, J. Geophys. Res.-Oceans, 119, 8029–8038, 2014. 2076, 2077, 2079, 2080, 2081, 2082, 2093
Lévêque, E., Toschi, F., Shao, L., and Bertoglio, J.-P.: Shear-improved Smagorinsky model for large-eddy simulation of wall-bounded turbulent flows, J. Fluid Mech., 570, 491–502, 2007. 2088
Monin, A. S. and Yaglom, A. M.: Statistical Fluid Mechanics, MIT Press, Boston, USA, 1975. 2076
Morel, P. and Larchevêque, M.: Relative dispersion of constant level baloons in the 200 mb general circulation, J. Atmos. Sci., 31, 2189–2196, 1974. 2075
Ohlmann, J. C., LaCasce, J., Washburn, L., Mariano, A. J., and Emery, B.: Relative dispersion observations and trajectory modeling in the Santa Barbara Channel, J. Geophys. Res.-Oceans, 117, C05040, doi:10.1029/2011JC007810, 2012. 2076
Okubo, A.: Some remarks on the Importance of the “Shear Effect” on Horizontal Diffusion, J. Ocean. Soc. Jap., 24, 60–69, 1968. 2077
Okubo, A.: Oceanic diffusion diagrams, Deep-Sea Res., 18, 789–802, 1971. 2075, 2077
Ollitrault, M., Gabillet, C., and De Verdière, C.: Open ocean regimes of relative dispersion, J. Fluid Mech., 533, 381–407, 2005. 2075

OSD
12, 2073–2096, 2015

Title Page
Abstract | Introduction
Conclusions | References
Tables | Figures
◂◂ | ▸▸
◂ | ▸
Back | Close
Full Screen / Esc
Printer-friendly Version
Interactive Discussion

Palatella, L., Bignami, F., Falcini, F., Lacorata, G., Lanotte, A. S., and Santoleri, R.: Lagrangian simulations and interannual variability of anchovy egg and larva dispersal in the Sicily Channel, J. Geophys. Res.-Oceans, 119, 1306–1323, 2014. 2077, 2080

Richardson, L. F.: Atmospheric diffusion on a distance-neighbour graph, Proc. R. Soc. Lond. A, 110, 709–737, 1926. 2075

Salazar, J. and Collins, L.: Two-particle dispersion in isotropic turbulent flows, Ann. Rev. Fluid Mech., 41, 405–432, 2009. 2075

Santamaria, F., De Lillo, F., Cencini, M., and G., B.: Gyrotactic trapping in laminar and turbulent Kolmogorov flow, Phys. Fluids, 26, 111901, doi:10.1063/1.4900956, 2014. 2087

Sawford, B.: Turbulent Relative Dispersion, Ann. Rev. Fluid Mech., 33, 289–317, 2001. 2075

Tonani, M., Pinardi, N., Dobricic, S., Pujol, I., and Fratianni, C.: A high-resolution free-surface model of the Mediterranean Sea, Ocean Sci., 4, 1–14, 2008, http://www.ocean-sci.net/4/1/2008/. 2079

OSD
12, 2073–2096, 2015

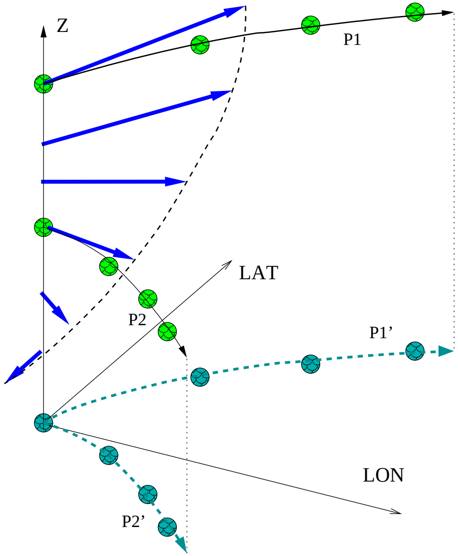

Figure 1. An illustration of the effect of vertical shear onto the mean horizontal dispersion of two particles, $P1$ and $P2$, initially separated along the vertical direction.

OSD
12, 2073–2096, 2015

The role of vertical shear on the horizontal oceanic dispersion

A. S. Lanotte et al.

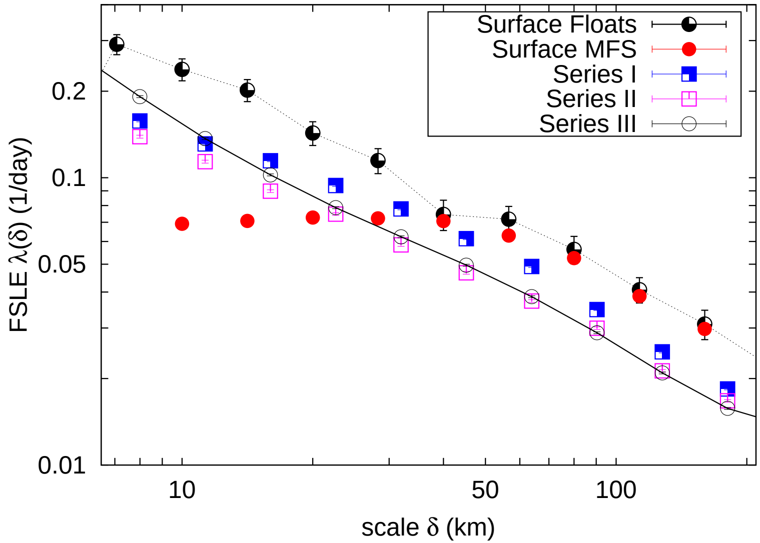

Figure 2. (Color online) log-log plot of the Finite-scale Lypaunov exponent $\lambda(\delta)$ versus the separation scale δ. Black filled circles: surface drifters; Red filled circles: MFS surface particles (both after Lacorata et al., 2014); Blue filled squares: Series I, that is MFS model for particle pairs at fixed depths; Purple empty squares: Series II, that is MFS model plus the 3-D KLM; Black empty circles with solid line: Series III, as Series II plus the 2-D KLM. Error bars, often smaller than the symbols themselves, are estimated from the standard deviation of the FSLE.

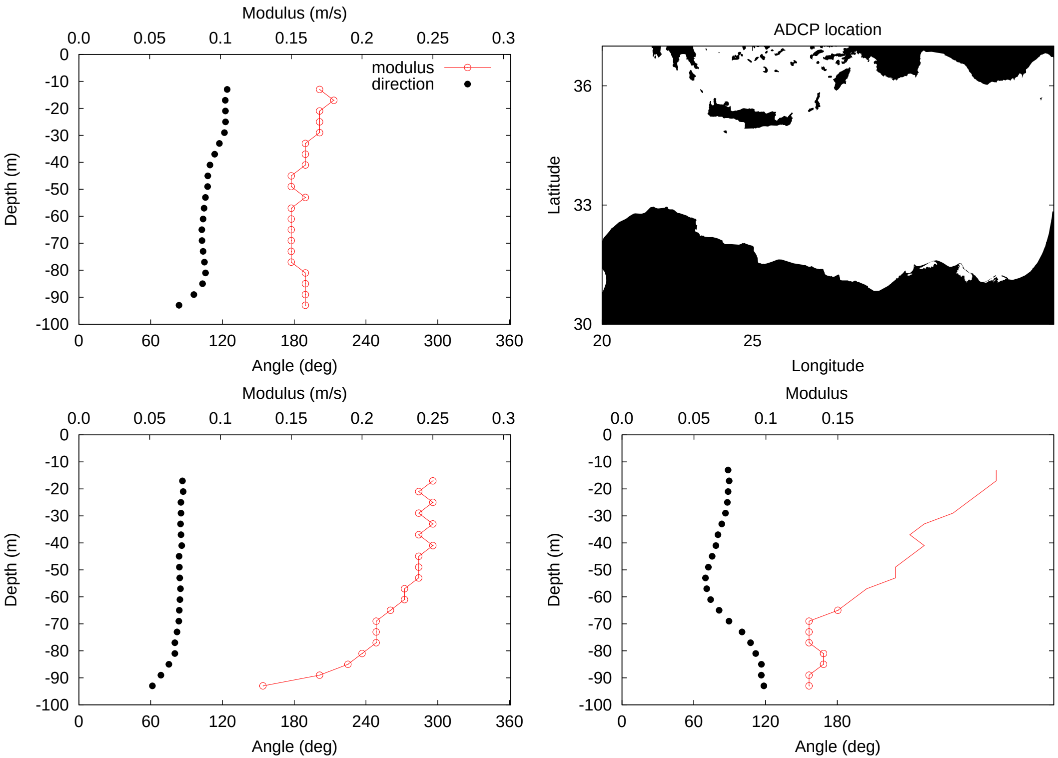

Figure 3. (Color online): Experimental current profiles of horizontal velocities. Empty red cirles: velocity modulus; black filled circles: direction from the north. In the top right panel, the small purple triangles indicate the ADCP locations.

OSD
12, 2073–2096, 2015

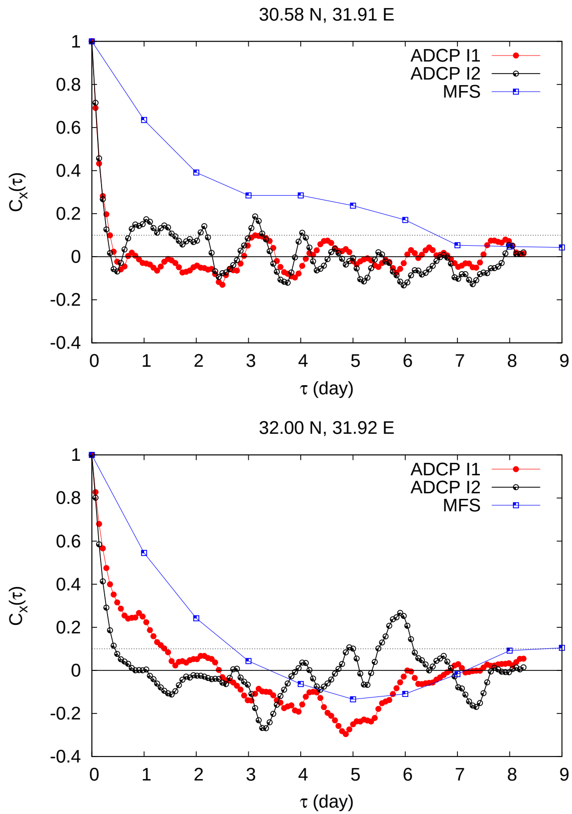

Figure 4. Log-lin plot of the velocity gradient autocorrelation functions versus the time lag. All data refer to the $\gamma'_x(t)$ component. Top plot is for the ADCP located at 0.58° N, 31.91° E; bottom plot is for the ADCP located at 32.00° N, 31.92° E. Symbols: Filled circles are for ADCP data of the period *I1*, February–April 1999; empty circles for ADCP data of the period *I2*, December 1999–February 2000; Squares are for the MFS data averaged over period *I1* and *I2*. Dotted lines indicate the value 0.1.

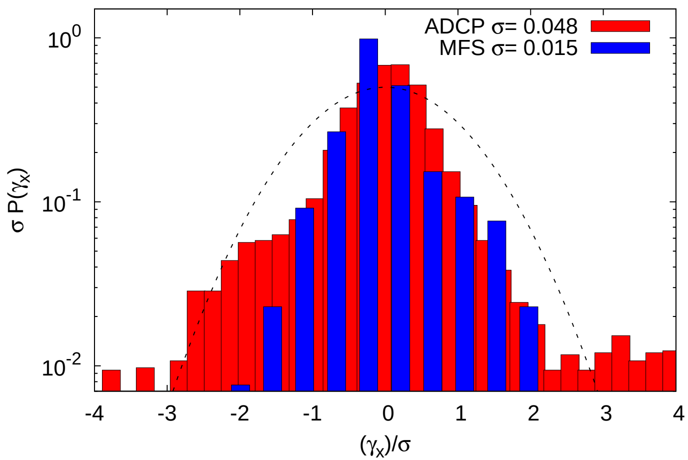

Figure 5. Lin-log plot of PDFs of the vertical shear component γ'_x. PDFs are normalised to have unit variance. Red boxes are for the ADCP data at location 31.92° N, 32.00° E; blue boxes are for the MFS data interpolated at the same location; the dashed curve is a normal distribution.

OSD
12, 2073–2096, 2015